AD-A171 723 ATOMIC LAYER EPITAXY OF III-V COMPOUNDS(U) UNIVERSITY OF SOUTHERN CALIFORNIA LOS ANGELES DEPT OF ELECTRICAL ENGINEERING P D DAPKUS ET AL. 18 AUG 86 53-4506-5066 1/1

UNCLASSIFIED N00014-85-K-0331 F/G 7/4 NL

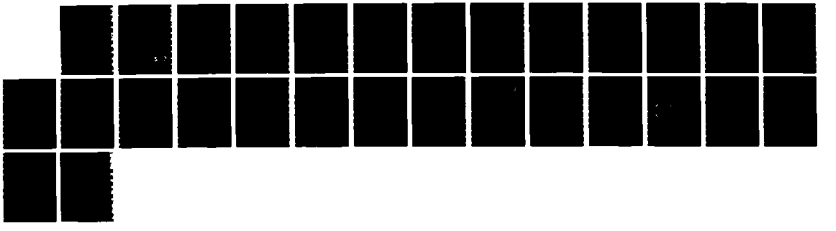

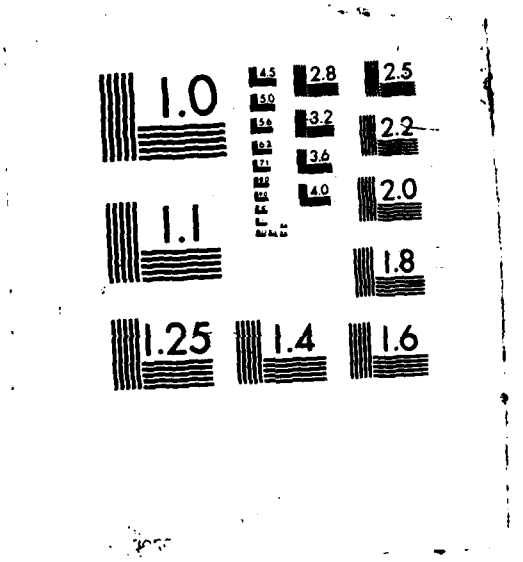
1.0
1.1
1.25
1.4
1.6
1.8
2.0
2.2
2.5
2.8
3.2
3.6
4.0
4.5
5.0
5.6
6.3
7.1
8.0
9.0
10.0
11.2
12.5
14.0
16.0
18.0
20.0
22.4
25.0
28.0
32.0
36.0

AD-A171 723

(12)

SECURITY CLASSIFICATION OF THIS PAGE

REPORT DOCUMENTATION PAGE

1a. REPORT SECURITY CLASSIFICATION: Not Classified	1b. RESTRICTIVE MARKINGS
2a. SECURITY CLASSIFICATION AUTHORITY: N/A	3. DISTRIBUTION/AVAILABILITY OF REPORT: Approved for public release; distribution unlimited.
2b. DECLASSIFICATION/DOWNGRADING SCHEDULE	
4. PERFORMING ORGANIZATION REPORT NUMBER(S): 53-4502-5066	5. MONITORING ORGANIZATION REPORT NUMBER(S)
6a. NAME OF PERFORMING ORGANIZATION: Univ. of Southern California; 6b. OFFICE SYMBOL (If applicable)	7a. NAME OF MONITORING ORGANIZATION: Office of Naval Research
6c. ADDRESS (City, State and ZIP Code): Dept. of EE/Electrophysics, ~~SSC-502~~ Los Angeles, CA 90089-0483	7b. ADDRESS (City, State and ZIP Code)
8a. NAME OF FUNDING/SPONSORING ORGANIZATION: Office of Naval Research; 8b. OFFICE SYMBOL (If applicable)	9. PROCUREMENT INSTRUMENT IDENTIFICATION NUMBER: N00014-85-K-0331
8c. ADDRESS (City, State and ZIP Code): Office of Naval Research, Arlington, Virginia 22217-5000	10. SOURCE OF FUNDING NOS. — PROGRAM ELEMENT NO. / PROJECT NO. / TASK NO. / WORK UNIT NO.
11. TITLE (Include Security Classification): ATOMIC LAYER EPITAXY OF III-V COMPOUNDS	
12. PERSONAL AUTHOR(S): Paul Daniel Dapkus, Curt Wittig, Susan Allen	
13a. TYPE OF REPORT: ANNUAL; 13b. TIME COVERED: FROM SEPT 85 TO AUG 86	14. DATE OF REPORT (Yr., Mo., Day): 86,08,18; 15. PAGE COUNT
16. SUPPLEMENTARY NOTATION	
17. COSATI CODES — FIELD / GROUP / SUB. GR	18. SUBJECT TERMS (Continue on reverse if necessary and identify by block number)
19. ABSTRACT (Continue on reverse if necessary and identify by block number)	
20 DISTRIBUTION/AVAILABILITY OF ABSTRACT: UNCLASSIFIED/UNLIMITED ☒ SAME AS RPT. ☐ DTIC USERS ☐	21 ABSTRACT SECURITY CLASSIFICATION
22a. NAME OF RESPONSIBLE INDIVIDUAL: Harriet Vigoren, Contract Administrator	22b. TELEPHONE NUMBER (Include Area Code): (213) 743-7762; 22c. OFFICE SYMBOL

DD FORM 1473, 83 APR — EDITION OF 1 JAN 73 IS OBSOLETE

ANNUAL REPORT

ONR Contract No. N00014-85-K-0331

ATOMIC LAYER EPITAXY

Principal Investigators:
S. D. Allen
P. D. Dapkus
C. Wittig

University of Southern California
Los Angeles, CA

Period Covered

June 1, 1984 to August 31, 1985

Introduction

This program is intended to develop a process for the growth of GaAs and related compounds by Atomic Layer Epitaxy (ALE). This report describes the efforts of the first 15 months of the program. The program involves fundamental studies of gas phase kinetics of the organometallic and hydrides to be used in the process as well as surface reaction studies to determine the surface of various organometallics. We have chosen in this program to effect ALE growth in a dense H_2 atomsphere. We believe that the reactivity of H_2 is important to the removal, by hydrogenation, of the alkyl radicals from the growing surface. To better understand the process we are pursuing fundamental information in two areas. First, basic measurements of the reactivity and reaction products of organometallics and hydrides and of photogenerated species with compound semiconductor surfaces are being undertaken that will determine the feasibility of using photoactivation and in thermal catalytic reactions in the gas phase to accomplish ALE. Second, epitaxial growth experiments are being performed to determine the feasibility of an ALE process employing photodecomposition of surface absorbed species as well as thermal catalytical reactions.

4.0. Current Status

4.1. Decomposition Kinetics of of TMGa and AsH_3

A study of the decomposition rates of TMGa and AsH_3 in H_2 has been undertaken. These studies are being done to determine the temperature range in which homogeneous (gas phase) reactions dominate the growth of GaAs and to examine the possibility of surface catalytic effects. The rates of decomposition are to be determined by analyzing the concentration of each

reactant in a mixture with hydrogen after the reactants had passed through a well confined hot region of a hot walled quartz reactor tube. The concentration of reactants at various temperatures are measured relative to the room temperature concentration by sampling infrared absorption spectroscopy. Isolated mixtures of TMGa or AsH_3 with H_2 are measured as well as mixtures of both AsH_3 and TMGa with H_2. The effect of specific surfaces such as GaAs substrates are measured by inserting large quantities in the hot zone to maximize the interaction of the surfaces with the gases. The results of these measurements are shown in Figs. 1 and 2. Note in Fig. 1 that TMGa decomposes homogeneously in the temperature range 380C-460C while AsH_3 decomposes in the range 475-600C. There is strong evidence that the AsH_3 decomposition is catalyzed the the quartz surface.

The presence GaAs wafers in the hot zone has little effect on the decomposition of TMGa while their presence accelerates the decomposition of AsH_3 at all temperatures. Additionally the decomposition of arsine is accelerated by the presence of TMGa vapor in the reactor. These results indicate the strong catalytic effects are operative in the decomposition of AsH_3 in an MOCVD reactor and that these reactioncs can be put to use in ALE growth.

The decomposition kinetics of TMGa and AsA_3 were analyzed assuming first order kinetics i.e.

$$\frac{dC(t)}{dt} = -K\ C(t) \qquad (1)$$

Where C is the concentration of the reactant in H_2 under study and K is the reaction rate constant. K is expcted to be of the form

$$K = K_0 \exp(-E_a/KT) \qquad (2)$$

Integrating (1) over the time interval in which the reactants are heated

($\Delta t = 1/v$), we have

$$\ln (C(T, \Delta t)/Co) = -K \Delta t \quad (3)$$

It then follows that

$$\ln K = \ln (\Delta t) + \ln \ln (Co/C(T,\Delta t)) \quad (4)$$
$$= -E_a/kT$$

We plot the log K as a function 1/T in Figs. 3 and 4. Note that an activation energy of $E_A \cong 60$ Kcal/mole is determined for TMGa decomposition. This agrees well with the known bond energy of the first CH_3 radical on TMGa. The activation energy of 34 Kcal/mole observed for AsH_3 is indicative of strong catalytic effects because the H-AsH_2 bond is known to be significantly larger. Note also that a lower activation energy is observed for the reaction on AsH_3 with GaAs surfaces. This is indicative of strong surface catalysis. These are the first successful measurements of the rates of decomposition of AsH_3 and TMGa and the first measurements of the reaction activation energies.

This data suggest that temperatures as low as 400C must be used to adsorb TMGa on GaAs in a H_2 atmosphere and avoid significant gas phase decomposition. Some means possibly thermal or optical must then be used to remove the CH_3 radicals. It should be noted that triethylgallium has beenemployed in MOMBE growth of GaAs with some success but will likely not be suitable in these studies because of its lower decomposition temperature.[1-4]

4.2 Epitaxial Growth Equipments

Several growth runs have been attempted to examine the ALE growth of GaAs in current reactors. While growth of GaAs has been achieved at temperatures as low 500C as by alternately exposing the wafer to TMGa and Ash_3, the quality of the films has not been easily assessed. Multilayer

AlGaAs/GaAs/AlGaAs structures have been grown in which the GaAs was grown by ALE. These structures await TEM examination to determine the growth rate per cycle of reactants. Owing to the long residence time of our reactor, excessive purge times between TMGa and AsH_3 exposures were required to avoid the possibility of conventional MOCVD deposition occurring from a gas mixture. Purge times in excess of one minute are thought to be necessary. This makes the time for growth of even thin layers excessive and long exposure of the surface during purge may result in surface decomposition. A new horizontal reactor vessel designed for ALE is being built that will be operated either at atmoshperic pressure or 0.1 atmospheres. This reactor will incorporate radiant heating to allow rapid temperature excursions. The rapid temperature changes may permit thermal decomposition of surface adsorbed specie. The residence time of the reactor will be as short a 1 sec.

4.3 Photoinitiated Processes

The technological goal in this part of our program is to develop a method for ALE using photodissociation as a means of preparing and manipulating reactive precursors. This can allow bonds to be broken selectively, so that the chemistry of the system is not constrained to follow the lowest energy (thermal) reaction pathways, thus opening the possibility of growth at reduced temperatures. Candidate molecules such as TMGa, PH_3, and AsH_3 can all be excited using UV radiation, and are known to decompose subsequent to photoexcitation. Their spectral signatures provide a means of selecting specific species in a gas mix, thus providing some control over radical concentrations, independent of the amount of starting material. However, dissociation mechanisms are not known, and even ptoduct

identification is sometimes elusive, as this area of photochemistry has not particularly been overrun during the past few decades.

Ideally, we would like to prepare controllable concentrations of species which can be used to systematically 'layer' surfaces. For example, can we dissociate AsH_3 to form a species which is stable in the gaseous phase but reacts readily at a surface? If AsH_3 photodissociation produces radicals which subsequently react with surrounding molecules to regenerate AsH_3, it may be difficult to get the reactive species formed by photodissociation to the surface. Thermochemical data for AsH_3 are sparse and questionable, and therefore it is hard to look up the answers to such questions. By analogy with NH_3 and PH_3,[5] one would naturally assume that the H-AsH_2 bond is the strongest, and the diatomic As-H bond is the weakest. However, putting numbers in is another matter. Also, the reaction of a species such as AsH_2 with TMGa is anyone's guess. It could be that products are formed which are either desirable or undesirable for growth; we simply don't know.

With the UV photons presently available from common off-the-shelf excimer lasers, it is possible to excite molecules such as TMGa and AsH_3 to energies very high above dissociation threshold. This is distinct from photoexcitation of lighter molecules, whose bonds are typically much stronger. For example, using the 193.3 nm output from an ArF laser, and assuming a H-AsH_2 bond strength of 24,500 cm^{-1},[6] the initially energized AsH_3 has an 'excess energy' ($E^{\dagger}=h\nu-D_0$) of 27,200 cm^{-1}. This energy must appear as relative translation of the fragments in the center-of-mass (c.m.) of the AsH_3, as well as AsH_2 internal excitation. Such a large value of $E^{\dagger}$ presents several possibilities. If the H-atom kinetic energy is ~6,000 cm^{-1} or less, the nascent AsH_2 will be excited above the thermodynamic threshold for subsequent decomposition to AsH+H. In the absence of forming

electronically metastable AsH_2, which we deem very unlikely,[7] this insures that AsH will be formed via a vibrational predissociation mechanism. Since the arsenic-hydrogen bond strength decreases in going from AsH_3 to AsH_2 to AsH, a species such as AsH is inhibited from reacting with an AsH_3 (or H_2) substrate. Reaction with TMGa is another matter altogether, and there are several viable reaction pathways. Another possibility is molecular elimination of H_2 from vibrationally excited AsH_2:

$$AsH_2 \rightarrow As+H_2 \qquad \Delta H \sim +6300\ cm^{-1}$$

In addition to the endothermicity, there will be a barrier for this reaction, and we have no way of estimiating its value. However, if the H-atom kinetic energies are small (but large enough to block dissociation via the AsH+H channel), the nascent $AsH_2^{\dagger}$ internal energy can be ~20,000 cm^{-1}, which can easily overcome the barrier associated with the 3-center elimination process.[8]

With the above considerations in mind, we have built an experiment which measures directly H-atom kinetic energies from processes such as those listed above. Our goal is to *(i)* find conditions under which photodissociation of III-V carriers produces well-characterized fragments, *(ii)* identify these species and their energies, *(iii)* measure and estimate reactivities, and *(iv)* apply this to the growth of GaAs using the MOCVD reactor described in the previous section. For the past few months, we have studied the photodissociation of PH_3,[8] and find an alarmingly small amount of H-atom kinetic energy. Here, $E^{\dagger}$ = 24,000 cm^{-1}, and we find that there is almost no PH_2 formed with < 8000 cm^{-1} of internal energy. The distribution is peaked near 16,000 cm^{-1}, and such *superexcitation* can be very instrumental in determining the fate of this species. In the next section, this

experiment is described and results are presented. Following this, we present our plans for future research.

Experimental Considerations and Arrangement

In any fragmentation process of the form $AB \rightarrow A + B$, the excess energy (E_{total}-D_0) is manifest as product translational and internal excitation. Thus, for cases in which a monoenergetic ensemble of excited molecules dissociates, knowledge of the c.m. kinetic energy distribution automatically gives the internal energy distribution for the *combined* fragments. For cases where it is certain that one of the products is in a specific state (e.g. the ground state), the internal energy distribution of the other fragment is determined uniquely. In this way, it is possible to obtain this information for species whose internal state distributions are difficult or impossible to measure directly (e.g. organometallics). For neutral fragments, both molecular beam[9] and sub-Doppler resolution optical techniques[10] have been used to determine c.m. kinetic energy distributions and the corresponding fragment internal state distributions. The molecular beam techniques are now sufficiently refined that vibrational and rotational structure are discernable under optimum conditions,[11] and the 'machines' reflect a technological evolution that spans several decades. For a particular reaction, increased kinetic energy resolution results in more detailed knowledge of the dynamics involved, with the degree to which one can resolve such distributions depending on the molecular system as well as the apparatus.

Experiments which use Doppler shifts to determine velocities can, in principle, be used to obtain accurate kinetic energy distributions. The availability of commercial lasers with MHz bandwidths makes this method an

attractive alternative to molecular beam technologies, since optical methods can be relatively simple and inexpensive. However, Doppler shift studies are confounded by the seemingly inherent difficulty of deconvoluting lineshapes to obtain kinetic energy distributions. Since Doppler shift measurements probe velocity *components*, many speeds can have the same velocity component in a particular direction, and thus it is very difficult to assign a unique distribution to an observed lineshape. In principle, this problem can be overcome by measuring only those species traveling in a direction parallel to the probe wave vector, $\mathbf{k}_{probe}$. Here, instead of measuring the projections of the different velocities onto $\mathbf{k}_{probe}$, the measurement gives the speed distribution *along* $\mathbf{k}_{probe}$, thereby allowing much higher kinetic energy resolution to be obtained. Here, we explain the method which we have developed which allows us to achieve this directional discrimination in our photodissociation studies of TMG, AsH_3, PH_3, etc.

In essence, we incorporate a sufficiently long delay between the firing of counterpropagating photolysis and probe lasers that only those fragments moving parallel to $\mathbf{k}_{probe}$ are sampled. The net result is a significant reduction in the complexity of the Doppler profile relative to the case of minimal delay between the two lasers. Specifically, H-atoms are detected via the Lyman-α transitions (121.6 nm)[12] following 193.3 nm photolysis. The generation of tunable vacuum ultraviolet (VUV) radiation by frequency tripling a tunable dye laser provides a convenient means for detecting H-atoms through 2-photon ionization.[13,14] By delaying the probe beam and thus reducing congestion in the lineshape, we find that the use of Doppler spectroscopy as a tool for determining kinetic energy distributions is facilitated, especially for polyatomic systems such as those of concern in our program. We are presently able to obtain spectra limited in resolution by the

bandwidth of the probe (~0.6 cm^{-1} at 121.6 nm), but it should be possible to increase this resolution by at least an order of magnitude without difficulty.

As shown in Fig. 5, the basic arrangement consists of separate photolysis and probe lasers counterpropagating through the ionization region of a time-of-flight (TOF) mass spectrometer. Translationally hot H-atoms are formed by dissociating the molecule of interest with the 193.3 nm output of an unpolarized ArF excimer laser. Mild focusing of the laser with a lens produces a rather collimated photolysis beam approximately 2 mm in diameter.

Using a probe beam composed of both VUV and UV photons, detection of the H-atoms is accomplished via 2-photon ionization. A XeCl excimer laser pumping a dye laser generates UV radiation, a small portion of which is frequency tripled upon focusing the laser output into a cell containing Kr. After passing through the cell, the radiation is focused into the ionization region of the TOF mass spectrometer with a LiF lens (f.l. = 40 mm). The tunable VUV radiation (~121.6 nm) excites H-atoms via the Lyman-α transitions, and photoionization of the excited atoms is achieved with the relatively intense 364.7 nm radiation (~5 mJ). The ionization process yields protons which are extracted (field strength ~ 330 V cm^{-1}), accelerated through 2.2 kV, and passed through a 1.5 m drift tube to a microchannel plate detector. Associated electronics collect and average the resulting signals. The experimental system utilizes a master clock, which controls the delay between the firing of the photolysis and probe lasers. Due to the jitter of the spark-gap triggered photolysis laser, the uncertainty in this delay is $\pm$ 50 ns. The 364.7 nm linewidth is approximately 0.25 cm^{-1}(measured with an etalon) making the corresponding VUV linewidth ~0.6 cm^{-1}. The exact value depends on the actual frequency spectrum of the fundamental beam, which was not determined.[15] Frequency scanning of the probe laser to obtain a 'Doppler profile' was done with a stepping motor, i.e. pressure-tuned etalon scanning was not used in the present experiments.

With the present experimental configuration, the probe beam functions as a small detection region centered in a larger 'cylinder of photolysis'. Figure 6 shows an idealized, 2-dimensional representation of the counterpropagating photolysis/probe arrangement. Although more exact experimental geometries will be analyzed in a future publication, a qualitative understanding of the role that delay plays in this particular experiment can be gained by examining Fig. 6.

For the moment, assume that photodissociation produces H-atoms uniformly throughout the shaded photolysis region indicated in Fig. 6, and consider the illustrative example of a diatomic molecule [e.g. HBr+hν $\rightarrow$ H+Br]. Although rather idealized compared to TMG, AsH_3, PH_3, etc., this example is useful since the photolysis laser will produce H-atoms with a very narrow speed distribution (~2.25×10^6 cm s^{-1}), with the atoms emanating from all points within the photolysis region. Photodissociation of polyatomics follows straightforwardly, and the spatially anisotropic velocity distributions associated with parallel and perpendicular transition moments and different laser polarizations can also be taken into account.[16] Here, we will discuss the simple case of an isotropic velocity distribution, which is expected to be a reasonable approximation for larger polyatomics. Now consider the effect which the delay between the photolysis and the probe lasers, τ_d, has on the H-atom Doppler shift spectrum observed at the detection region. The concentric circles in Fig. 6 identify the spatial regions from which H-atoms traveling at 2.25×10^6 cm s^{-1} *must* originate if they are to arrive at the detection point at the indicated delays. For short delays, e.g. $\tau_d < 50$ ns, a full distribution of H-atom velocity components along $\mathbf{k}_{probe}$ will be observed at the detection region, since the entire 'circle of origin' is contained within the photolysis region. Consequently, a rather full Doppler profile will be obtained.

At longer delays the situation changes because the photolysis region does not fully envelope the 'circle of origin'. As depicted in Fig. 6, those spatial regions which

would produce H-atoms possessing significant velocity components *perpendicular* to $\mathbf{k}_{probe}$ do not contribute H-atoms to the detection region, since no photolysis occurs in those regions. Therefore, the Doppler profile exhibits a large reduction of intensity at frequencies corresponding to little or no Doppler shift. Inspection of Fig. 6 suggests that this effect will become more pronounced as τ_d increases. By comparing the places where the 100 and 150 ns circles intersect the photolysis region, it can be seen that the maximum velocity component perpendicular to $\mathbf{k}_{probe}$ *decreases* as τ_d goes from 100 to 150 ns. As a result, the hole in the observed Doppler profile widens.

An experimental verification is shown in Fig. 7 for the case of HBr. Photodissociation does not lead to spatially isotropic fragment velocities, and the observed Doppler lineshape for τ_d = 30 ns is characteristic of a perpendicular electronic transition and rapid dissocation.[16] Nevertheless, Fig. 6 acts as a qualitative guide to understanding the experimental results. The Doppler profile undergoes a dramatic change with delay, and the lineshape evolves into two peaks corresponding to H-atoms whose velocities are nearly parallel to $\mathbf{k}_{probe}$, the resolution at τ_d = 280 ns being limited by the dye laser system (~0.6 cm^{-1} at 121.6 nm). The asymmetries and random fluctuations are due to inexact spatial alignment of the laser beams and spark gap jitter; the true S/N is high, even at long delays.

The case of HBr photolysis is special in the sense that the H-atoms are nearly monoenergetic. The main point we wish to emphasize with this example concerns using this technique to obtain kinetic energy distributions. Examination of the τ_d = 30 ns spectrum in Fig. 7 reveals a Doppler width of approximately 12 cm^{-1}, which is in accord with the maximum possible speed of the H-atom. However, it is not immediately apparent from the observed lineshape that the speed **distribution** for the H-atom is narrow. On the

other hand, the 280 ns spectrum yields not only the maximum speed, but also clearly illustrates the narrowness of the speed distribution along $\mathbf{k}_{probe}$. Of course, this result is consistent with what one would expect for the photolysis of an especially simple case like HBr. However, when photolyzing a larger molecule, *a priori* knowledge of the H-atom speed distribution is no longer possible, because of vibrational and rotational degrees of freedom in the remaining fragment. Yet, the principle which led to the simplification of the Doppler profile in the case of HBr still applies.

Next, and more importantly, we examined the photodissociation of PH_3 (i.e. $PH_3 + h\nu(193.3\ nm) \rightarrow PH_2 + H$). The absorption cross section and excess energy are both large, and the experiment presents no difficulty. The dynamics of this reaction have been discussed previously, and there is evidence suggesting that PH_2 molecules may be formed with a large amount of vibrational energy.[17] In the present set of experiments, we determined how the Doppler profile varies with τ_d, since this information is very useful for understanding the reaction mechanism.

Figure 8 presents H-atom Doppler profiles for the 193.3 nm photolysis of PH_3 at several different photolysis/probe delays. As shown, the general contour of the lineshape changes upon going to longer delays, but the effect is not nearly as dramatic as in the case of HBr, even though delays of up to 500 ns were used in the case of PH_3. Each of the spectra in Figs. 7 and 8 is normalized separately, and the absolute peak intensity of the τ_d = 500 ns spectrum in Fig. 4 is much smaller than that for τ_d = 50 ns. Also, the long delay spectrum appears broader (FWHM) than the short delay spectrum. These observations can be reconciled by noting that the long delay discriminates against H-atoms whose velocities are not parallel to $\mathbf{k}_{probe}$, as

described above, and the apparent broadening of the lineshape occurs because the 'wings' of the spectrum are enhanced relative to the middle. Moreover, despite the long delay, signal still persists throughout the Doppler profile *not* as a result of insufficient discrimination, but because the spectrum reflects the speed distribution along $\mathbf{k}_{probe}$. We presently attach no significance to the small bumps in the τ_d = 500 ns spectrum; future work at higher resolution will be used to sort out such details.

Thermodynamic considerations indicate that the amount of energy available to the products is comparable for the cases of HBr and PH_3.[18] However, a comparison between Figs. 7 and 8 shows that H-atoms arising from PH_3 photolysis travel much more slowly than those from HBr photolysis, *at least along the direction of* $\mathbf{k}_{probe}$. The ramifications of this in terms of the PH_2 internal energy distribution are quite interesting. If the PH_2 which gives rise to the observed H-atom is formed in its electronic ground state, and the PH_3 disssociation energy is close to the reported value of 29,700 cm^{-1},[18] then the *minimum* amount of PH_2 internal energy is ~8000 cm^{-1} and a significant fraction of the PH_2 contains at least 15,000-18,000 cm^{-1} of internal energy, most likely in the form of bending motion.[17]

The experimental technique described above offers promise as a method for studying a wide variety of the molecular systems of importance to our program. The speed with which we can take data will allow us to peruse candidate molecules with definitive fragment identification, and energy resolution which is quite adequate for our purposes. For the case of H-atom detection, narrowing the VUV bandwidth may allow one to infer vibrational and/or electronic state distributions of the remaining fragment. The fact that the spectroscopy involved is exclusively that of atomic

hydrogen makes this technique especially attractive. Since the H-atom is formed in its ground state, obtaining its kinetic energy distribution leads to an inference of the internal energy distribution for the remaining fragment, even for species whose internal state distributions cannot be measured directly. This includes nearly all of the important radicals produced by the photodissociation of organometallics and group 5 hydrides.

5.4 Photoinitiated Processes

We will finish the work with PH_3, and then use the arrangement described above to study the photodissociation of AsH_3 and TMGa. Nascent reaction products will be identified, and we will determine both the internal and c.m. kinetic energy distributions. This will be done for several convenient laser wavelengths. These experiments do not take very long, and we should be able to finish the measurements in approximately 3 months. We will aim toward making highly reactive radicals (As, AsH) and determining the appropriate photolysis wavelength(s), and fragment distributions.

As our studies progress, we will be able to identify the appropriate conditions to produce potentially useful photoactivated species for ALE. It will then be possible to examine in the ESCA/Growth system the adsorbates produced from the photoproduced species. One can envision a geometrical progression of experiments in which the effects of reactor pressure, substrate temperature, and carrier gas treatment of adsorbates are considered. It is, however, premature to specify these directions until the basic measurements are completed and assessed. It is sufficient to state that a close interaction between the groups working on this project exists, and that positive results will be exploited as quickly as possible.

In our work so far, we found that measuring reaction rates of radicals such as PH_2 was not trivial, because of the large amount of internal excitation which had to be removed in order to have a thermalized sample. Nevertheless, in a real growth environment the reactions of such highly excited species is very important. In order to assess the reactivity of the highly excited radicals which we now know are produced by photodissociation, we will work with binary species such as TMGa••AsH_3.

Because of the Lewis-acid/Lewis-base nature of such species, we know that a small equilibrium concentration of these complexes exist at modest temperatures. Using methods which are common in our laboratory,[ref] we will prepare high concentrations of these species by expanding gas mixtures from a pulsed supersonic nozzle. Excitation/dissociation of one of the molecular constituents can then be used to prepare highly reactive species in close proximity to one another. For example, if the AsH_3 constituent of a weakly bonded complex is dissociated, the resulting $TMGa \cdot\cdot AsH_2$ transient will evolve to products from the specific geometry dictated by the equilibrium structure of the complex. These studies can be done without introducing complicated secondary collisions, and we will be able to determine the reaction products in a clean environment. It is quite possible that such a reaction will lead to a metastable species in which Ga and As are in the proper 1:1 stoichiometric ratio.

Note that this idea of working with species which are attached to one another is very close to the physical situation of photodissociating species which are adsorbed or chemisorbed on surfaces.

REFERENCES

1. J. Nishizawa, H. Abe, and T. Kurabayashi, J. Electrochem. Soc. **132**, 1197 (1985).
2. S.M. Bedair, M.A. Tischler, T. Katsuyama, and N.A. El-Masry, Appl. Phys. Lett. **47**, 51 (1985).
3. G.B. Stringfellow, Trip Report for 12th International Symposium on GaAs and Related Compounds; M. Yoder, private communication.
4. M. Yoshida, H. Watanabe, and F. Uesugi, J. Electrochem. Soc. **132**, 677 (1985).
5. H. Okabe, *Photochemistry of Small Molecules*, Wiley, NY, 1978.
6. S. Benson, private communication, also see S. Benson, *Thermochemical Kinetics, 2nd ed.*, Wiley, NY, 1976.
7. In all of our experiments to date, we do not detect significant PH_2 electronic excitation following the 193 nm photolysis of PH_3. D. Baugh, B. Koplitz, Z. Xu, and C. Wittig, Chem. Phys. Lett. (1986).
8. J. Caballero and C. Wittig, J. Chem. Phys. **82**, 1332 (1985).
9. A.M. Wodtke and Y.T. Lee, J. Phys. Chem. **85**, 4744 (1985).
10. E.J. Murphy, J.H. Brophy, and J.L. Kinsey, J. Chem. Phys. **74**, 331 (1981).
11. M. Faubel, J. Frick, G. Kraft, and J.P. Toennies, Chem. Phys. Lett. **116**, 12 (1985).
12. C.E. Moore, Atomic Energy Levels, Vol. I (Nat'l. Bur. Std. (U.S.), 1970).
13. H. Zacharias, H. Rottke, J. Danon, and K.H. Welge, Optics Comm. **37**, 15 (1981).
14. R. Schmiedl, H. Dugan, W. Meier, and K.H. Welge, Z. Phys. A **304**, 137 (1982).
15. J.C. Miller, R.N. Compton, and C.D. Cooper, J. Chem. Phys. **76**, 3967 (1982).
16. R.N. Zare and D.R. Herschbach, Proc. IEEE **51**, 173 (1963).
17. C.L. Sam and J.T. Yardley, J. Chem. Phys. **69**, 4621 (1978).
18. G. DiStefano, M. Lenzi, A. Margani, A. Mele, and C.N. Xuan, J. Photochem. **7** (1977). 335.

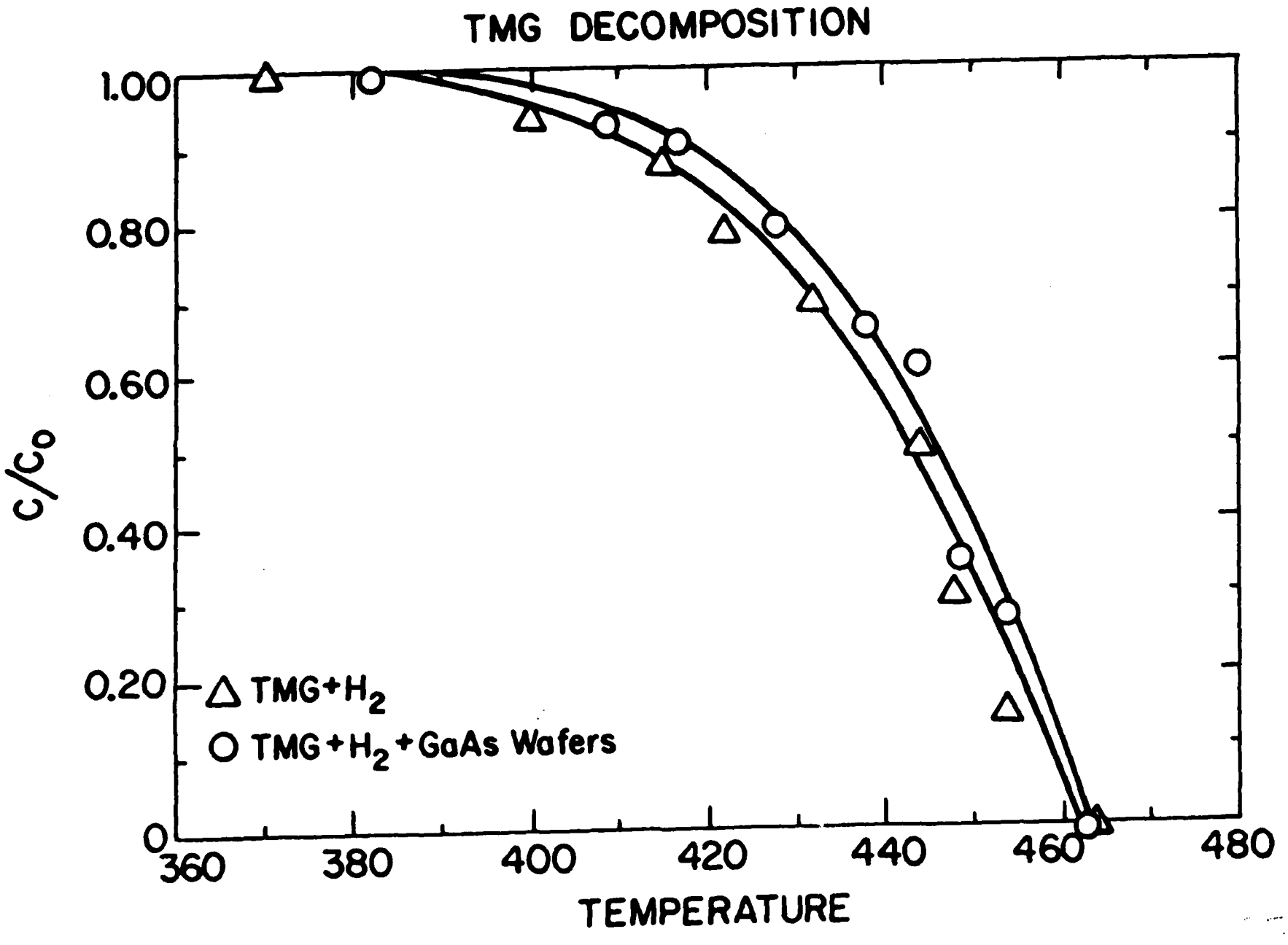
TMG DECOMPOSITION
1.00
0.80
0.60
0.40
0.20
0
C/C₀
△ TMG+H₂
○ TMG+H₂+GaAs Wafers
360
380
400
420
440
460
480
TEMPERATURE

Figure 1

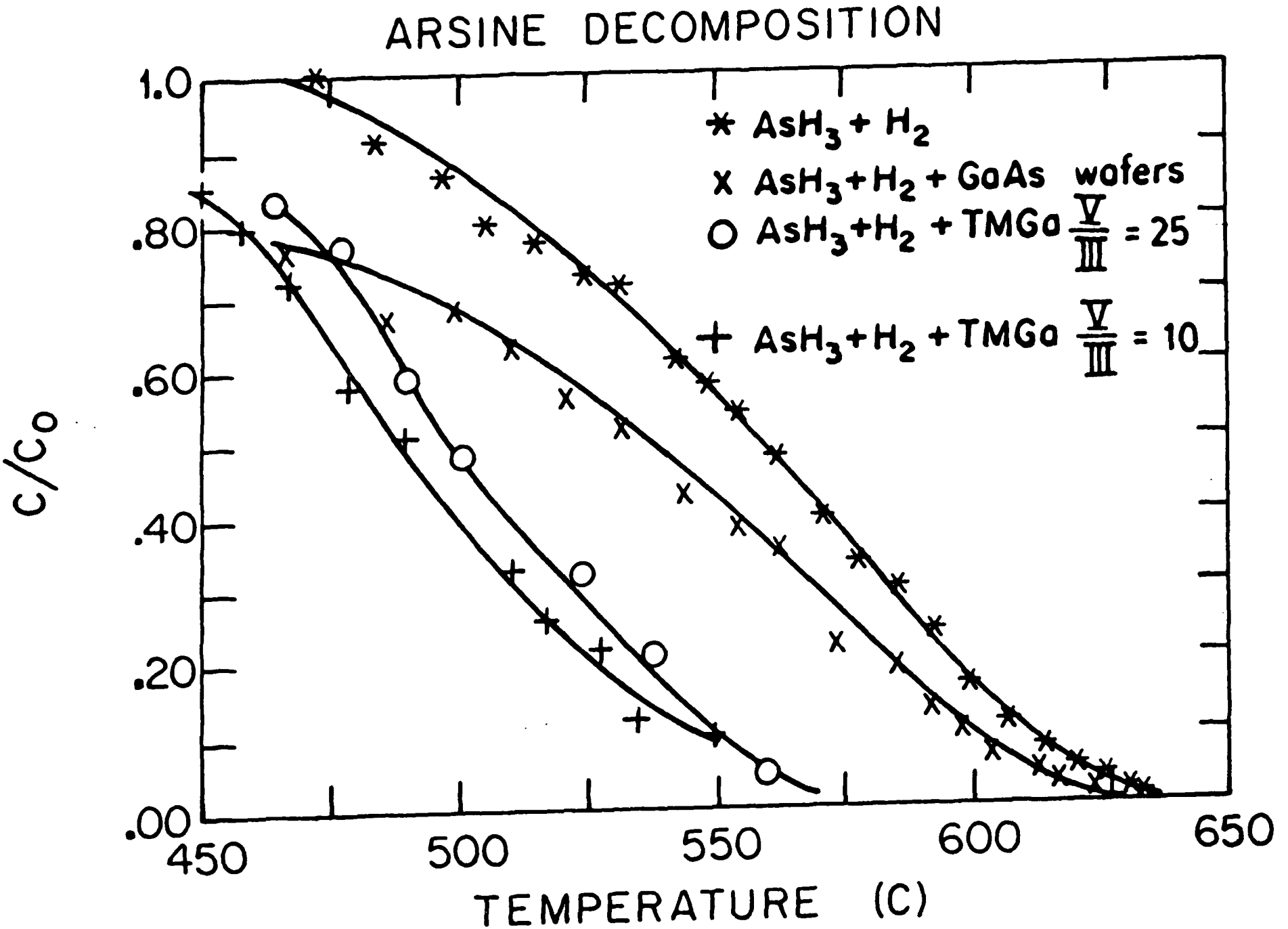
ARSINE DECOMPOSITION
1.0
.80
.60
.40
.20
.00
C/Co
450
500
550
600
650
TEMPERATURE (C)
* AsH3 + H2
X AsH3+H2 + GoAs wafers
O AsH3+H2 + TMGo V/III = 25
+ AsH3+H2 + TMGo V/III = 10

Figure 2

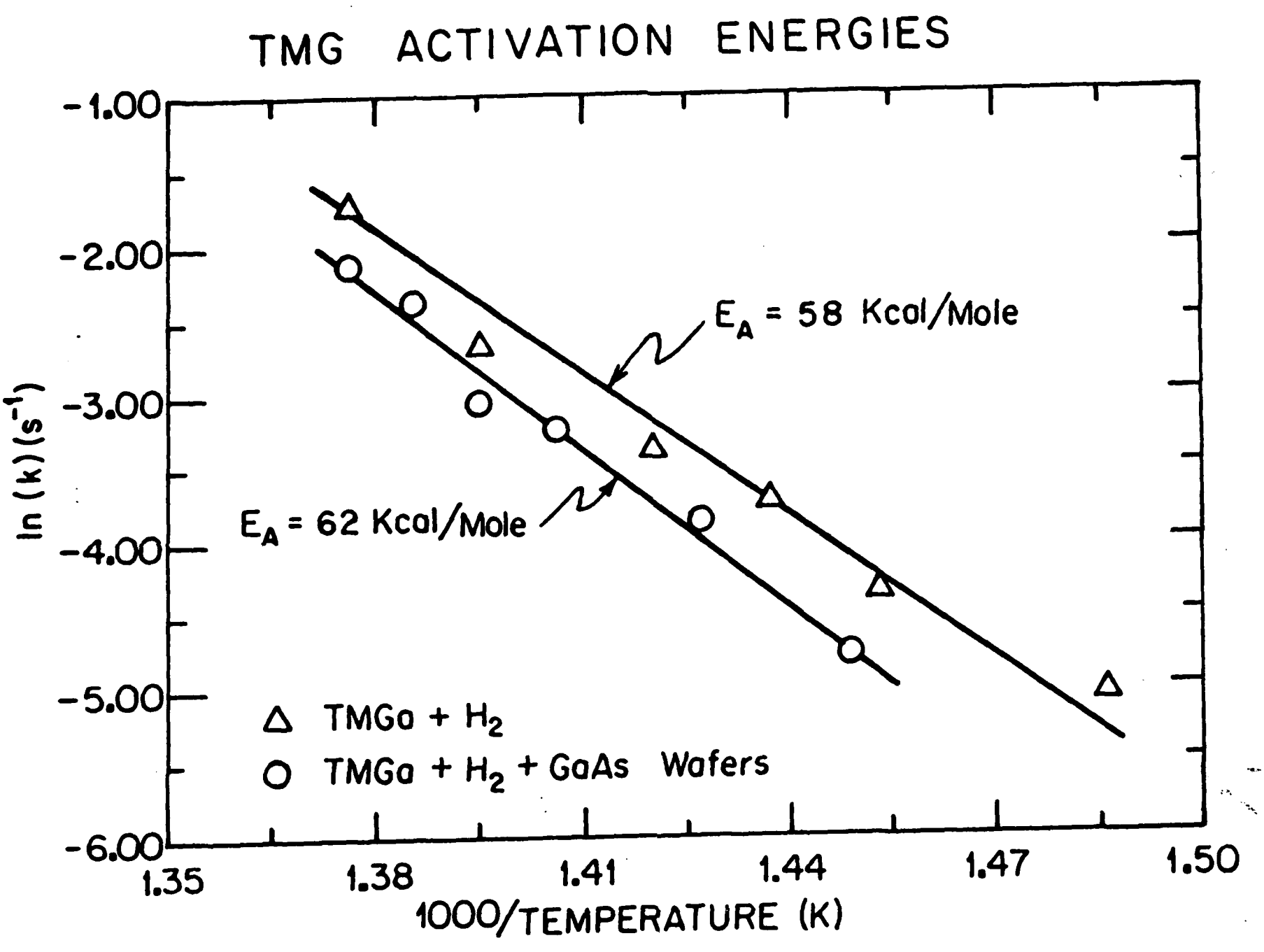
TMG ACTIVATION ENERGIES
-1.00
-2.00
-3.00
-4.00
-5.00
-6.00
ln (k)(s⁻¹)
E_A = 58 Kcal/Mole
E_A = 62 Kcal/Mole
△ TMGa + H2
○ TMGa + H2 + GaAs Wafers
1.35
1.38
1.41
1.44
1.47
1.50
1000/TEMPERATURE (K)

Figure 3

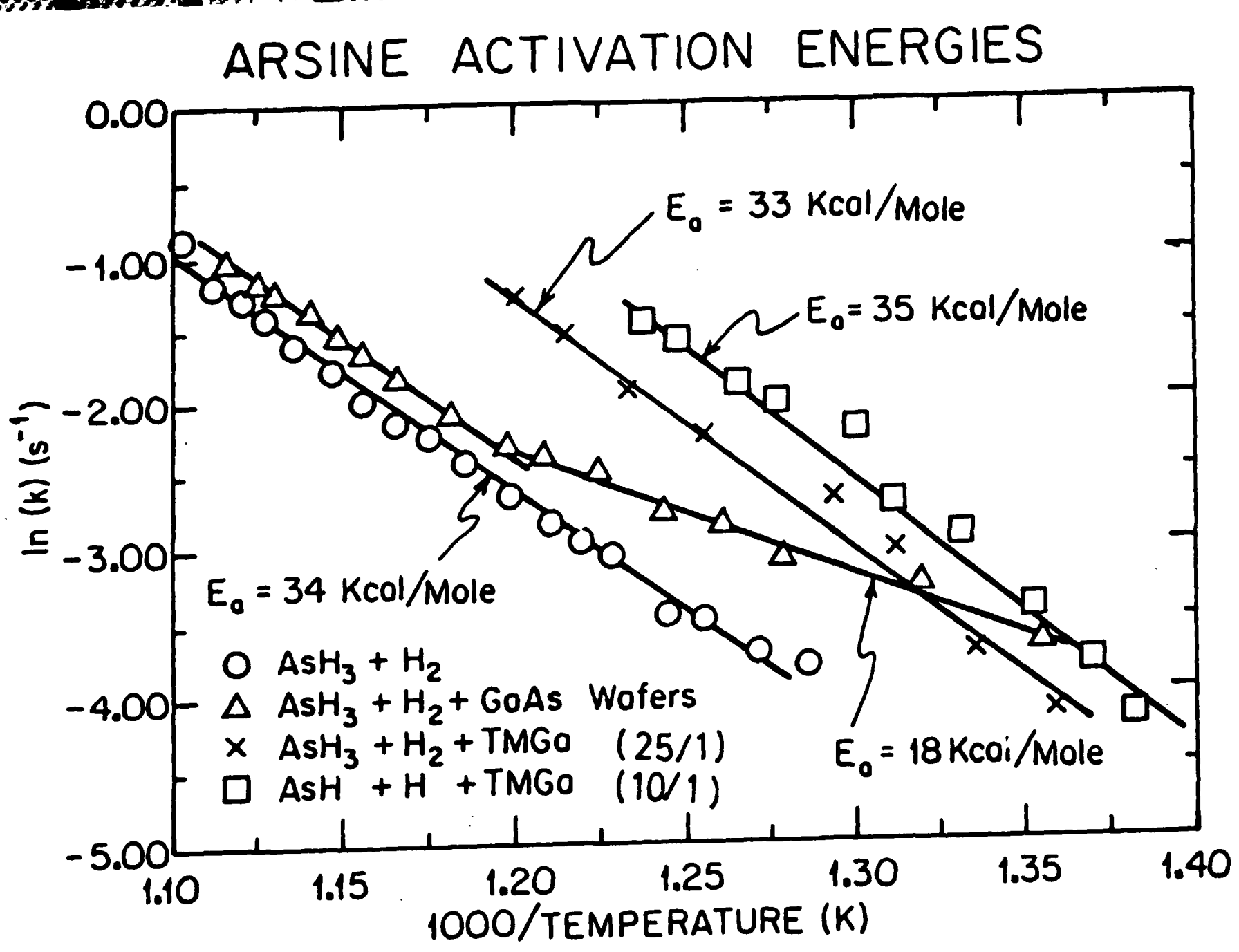
ARSINE ACTIVATION ENERGIES
0.00
-1.00
-2.00
-3.00
-4.00
-5.00
ln (k) (s⁻¹)
1.10
1.15
1.20
1.25
1.30
1.35
1.40
1000/TEMPERATURE (K)
E_a = 33 Kcal/Mole
E_a = 35 Kcal/Mole
E_a = 34 Kcal/Mole
E_a = 18 Kcal/Mole
O AsH3 + H2
Δ AsH3 + H2 + GaAs Wafers
× AsH3 + H2 + TMGa (25/1)
□ AsH + H + TMGa (10/1)

Figure 4

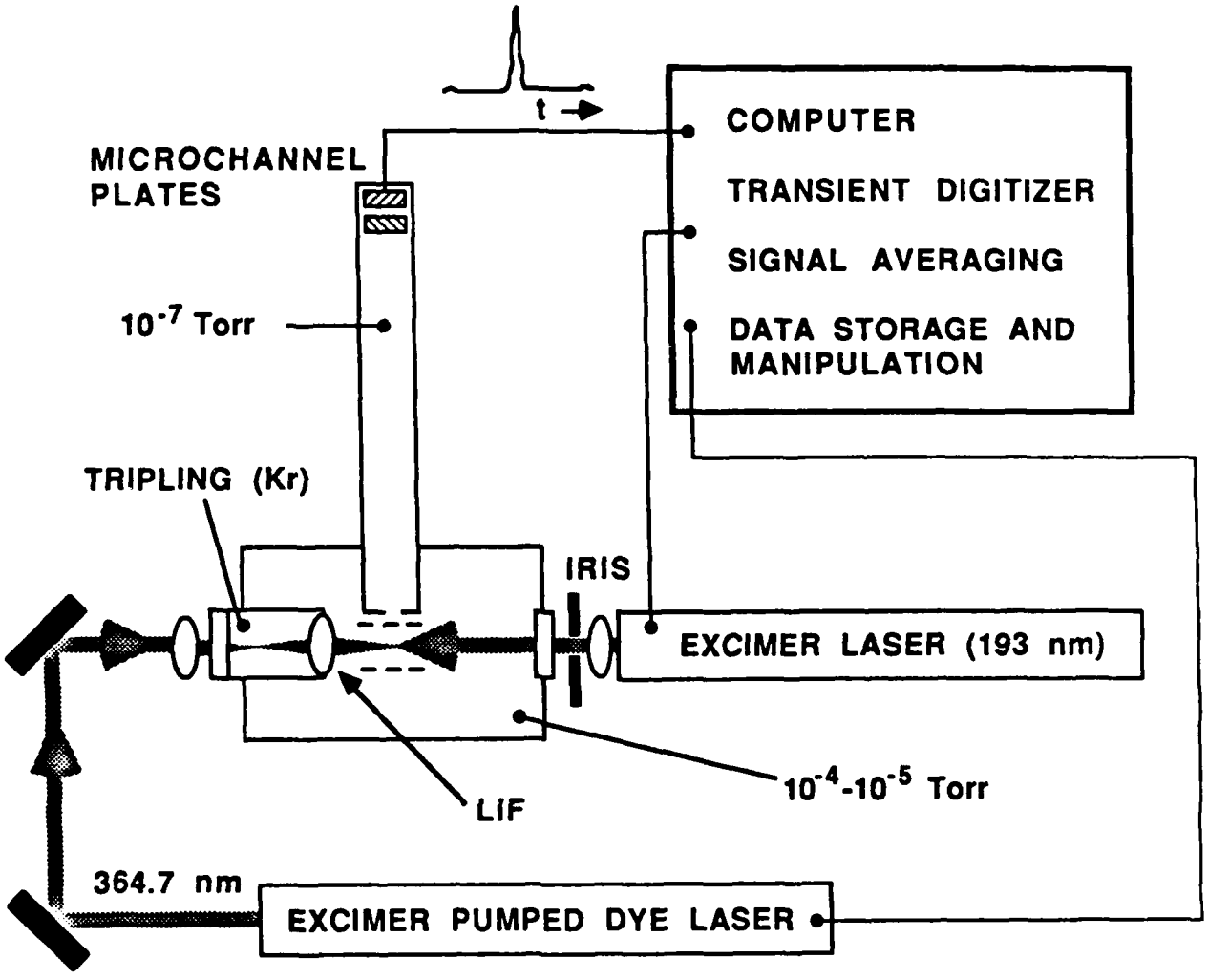

FIG. 5. Schematic diagram of the experimental apparatus.

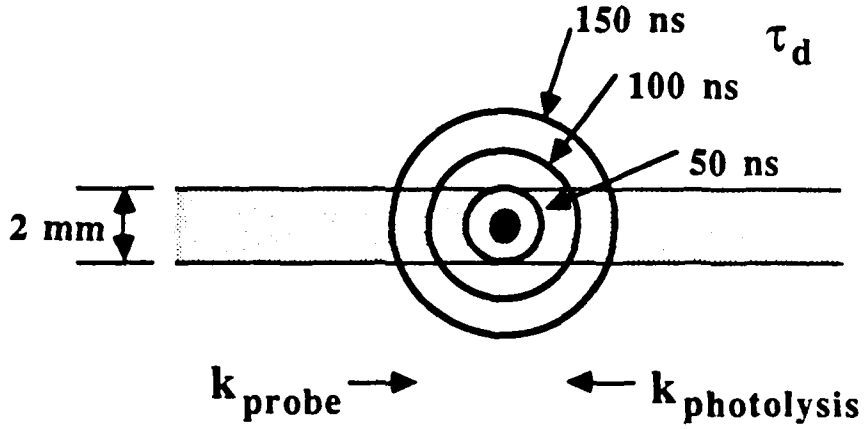

FIG. 6. An idealized, 2-dimensional representation of the photolysis/probe region. The shaded area indicates where photolysis occurs, while the dark center marks the probe detection region. The concentric circles identify the positions in space from which H-atoms travelling at 2.25×10^6 cm s^{-1} must originate in order to arrive adetection region at the indicated delay, τ_d.

FIG. 7. Doppler profiles for H-atoms (Lyman-α, 121.6 nm) produced by the 193.3 nm photolysis of HBr. The delay between the photolysis and probe lasers, τ_d, has an uncertainty of ± 50 ns.

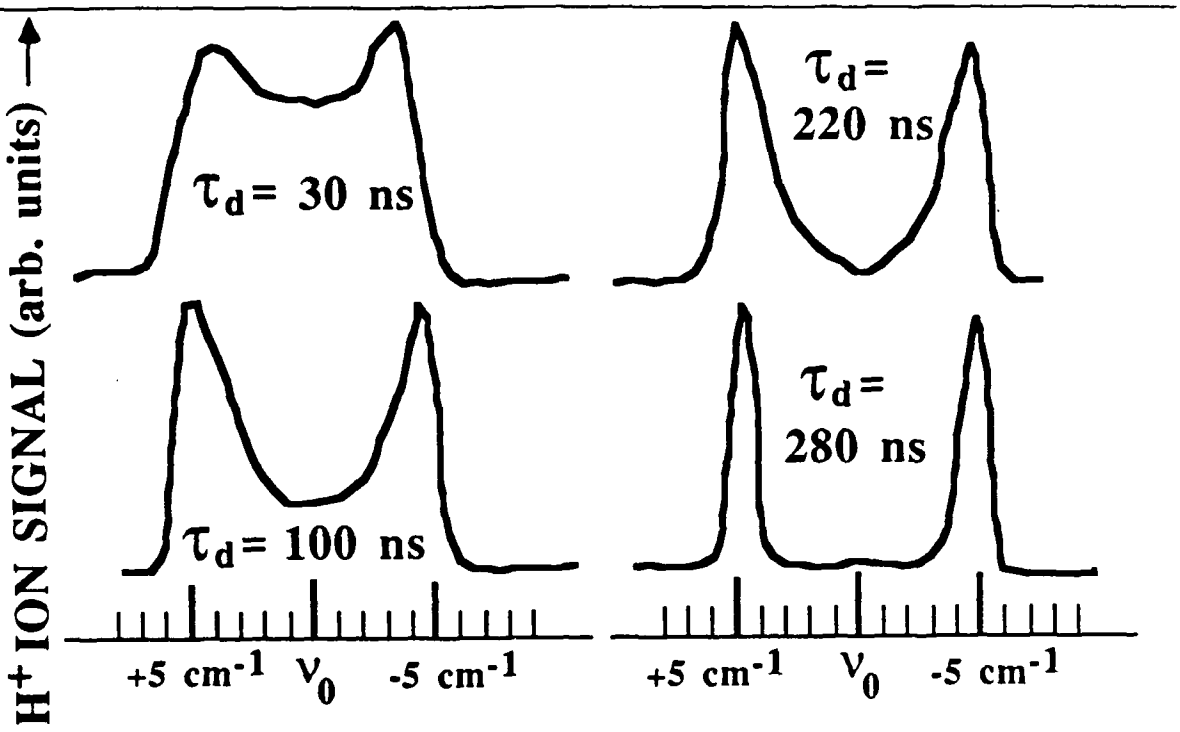

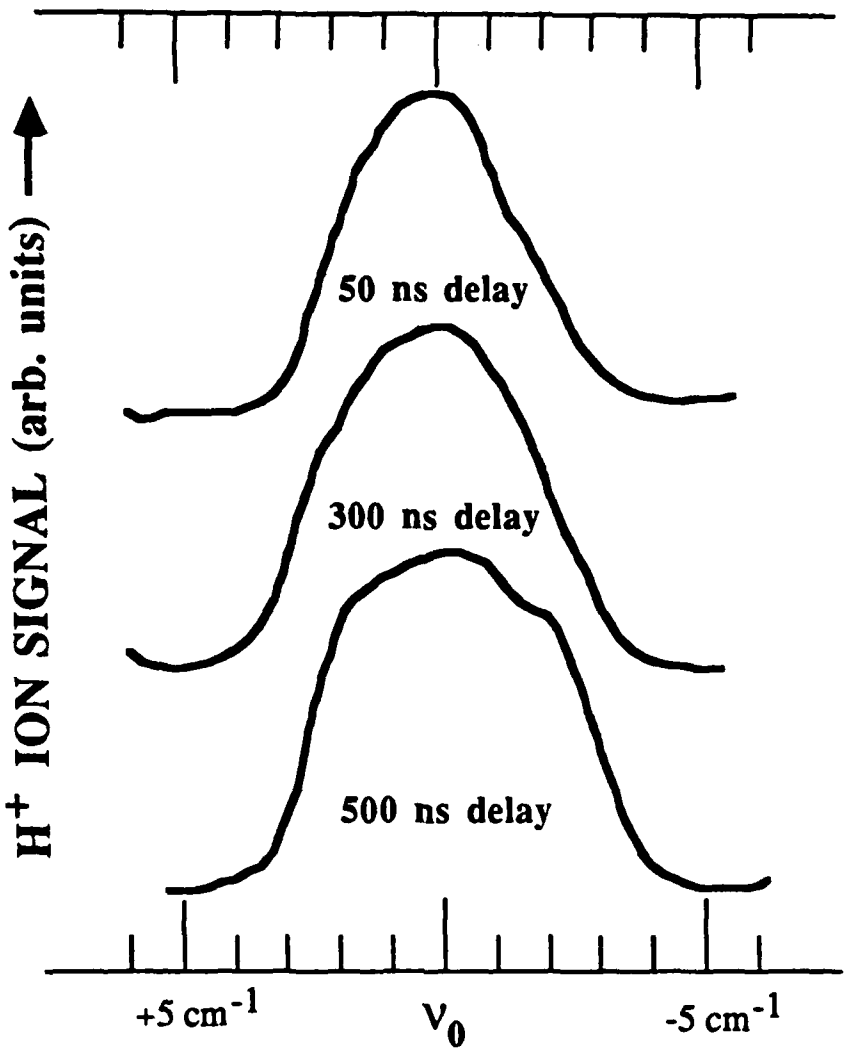

FIG. 8. Doppler profiles for H-atoms (Lyman-α, 121.6 nm) produced by the 193.3 nm photolysis of PH_3. The delay between the photolysis and probe lasers, τ_d, has an uncertainty of ± 50 ns.

END

10-86

DTIC